High-Resolution analysis of the Peptidoglycan composition in Streptomyces coelicolor

Aart, L.T. van der; Spijksma, G.K.; Harms, A.C.; Vollmer, W.; Hankemeier, T.; Wezel, G.P. van

JB Accepted Manuscript Posted Online 30 July 2018
J. Bacteriol. doi:10.1128/JB.00290-18

High-resolution analysis of the peptidoglycan composition in *Streptomyces coelicolor*

Lizah T. van der Aart[1], Gerwin K. Spijksma[2], Amy Harms[2], Waldemar Vollmer[3], Thomas Hankemeier[2] and Gilles P. van Wezel[1,4]*

1: Molecular Biotechnology, Institute of Biology, Leiden University, Sylviusweg 72, P.O. Box 9502, 2300RA Leiden, The Netherlands

2: Division of Analytical Biosciences, Leiden Academic Centre for Drug Research, Leiden University, The Netherlands

3: Centre for Bacterial Cell Biology, Institute for Cell and Molecular Biosciences, Newcastle University, Newcastle upon Tyne, United Kingdom

4: Department of Microbial Ecology, Netherlands, Institute of Ecology (NIOO-KNAW) Droevendaalsteeg 10, Wageningen 6708 PB, The Netherlands

*Corresponding author. Tel: +31 715274310; Email: g.wezel@biology.leidenuniv.nl

Running title: Peptidoglycan analysis of *Streptomyces coelicolor*

Keywords: Cell wall; Streptomyces; Mass spectrometry; Multicellular growth; Sporulation; Programmed Cell Death

ABSTRACT

The bacterial cell wall maintains cell shape and protects against bursting by the turgor. A major constituent of the cell wall is peptidoglycan (PG), which is continuously modified to allow cell growth and differentiation through the concerted activity of biosynthetic and hydrolytic enzymes. Streptomycetes are Gram-positive bacteria with a complex multicellular life style alternating between mycelial growth and the formation of reproductive spores. This involves cell-wall remodeling at apical sites of the hyphae during cell elongation and autolytic degradation of the vegetative mycelium during the onset of development and antibiotic production. Here, we show that there are distinct differences in the cross-linking and maturation of the PG between exponentially growing vegetative hyphae and the aerial hyphae that undergo sporulation. LC-MS/MS analysis identified over 80 different muropeptides, revealing that major PG hydrolysis takes place over the course of mycelial growth. Half of the dimers lacked one of the disaccharide units in transition-phase cells, most likely due to autolytic activity. De-acetylation of MurNAc to MurN was particularly pronounced in spores, and strongly reduced in sporulation mutants deleted for *bldD* or *whiG*, suggesting that MurN is developmentally regulated. Taken together, our work highlights dynamic and growth phase-dependent changes in the composition of the PG in *Streptomyces*.

IMPORTANCE

Streptomycetes are bacteria with a complex lifestyle, which are model organisms for bacterial multicellularity. From a single spore a large multigenomic, multicellular mycelium is formed, which differentiates to form spores. Programmed cell death is an important event during the onset of morphological differentiation. In this work we provide new insights into the changes in the peptidoglycan composition and over time, highlighting changes over the course of development and between growing mycelia and spores. This revealed dynamic changes in the peptidoglycan when the mycelia aged, with extensive PG hydrolysis and in particular an increase in the proportion of 3-3-cross-links. Additionally, we identified a

49 muropeptide that accumulates predominantly in the spores, and may provide clues towards
50 spore development.
51

INTRODUCTION

Peptidoglycan (PG) is a major component of the bacterial cell wall. It forms a physical boundary that maintains cell shape, protects cellular integrity against the osmotic pressure and acts as a scaffold for large protein assemblies and exopolymers (1). The cell wall is a highly dynamic macromolecule that is continuously constructed and deconstructed to allow for cell growth and to meet environmental demands (2). PG is built up of glycan strands of alternating *N*-acetylglucosamine (GlcNAc) and *N*-acetylmuramic acid (MurNAc) residues that are connected by short peptides to form a mesh-like polymer. PG biosynthesis starts with the synthesis of PG precursors by the Mur enzymes in the cytoplasm and cell membrane, resulting in lipid II precursor, undecaprenylpyrophosphoryl-MurNAc(GlcNAc)-pentapeptide. Lipid II is transported across the cell membrane by MurJ and/or FtsW/SEDS proteins and the PG is polymerized and incorporated into the existing cell wall by the activities of glycosyltransferases and transpeptidases (3-5).

The Gram-positive model bacterium *Bacillus subtilis* grows via lateral cell-wall synthesis followed by binary fission; in addition, *B. subtilis* forms heat- and desiccation-resistant spores (6, 7). By contrast, the vegetative hyphae of the mycelial *Streptomyces* grow by extension of the hyphal apex and cell division results in connected compartments separated by cross-walls (8-10). This makes *Streptomyces* a model taxon for bacterial multicellularity (11). Multicellular vegetative growth poses different challenges to *Streptomyces*, including the synthesis of many chromosomes during vegetative growth and separation of the nucleoids in the large multi-genomic compartments during cross-wall formation (12, 13). In submerged cultures, streptomycetes typically form complex mycelial networks or pellets (14). On surface-grown cultures, such as agar plates, these bacteria develop a so-called aerial mycelium, whereby the vegetative or substrate mycelium is used as a substrate. The aerial hyphae eventually differentiate into chains of spores, a process whereby many spores are formed almost simultaneously, requiring highly complex coordination of nucleoid segregation and condensation and multiple cell division (12, 15, 16). Streptomycetes have an unusually complex cytoskeleton, which plays a role in polar growth

and cell-wall stability (17, 18). Mutants that are blocked in the vegetative growth phase are referred to as bald or *bld*, for lack of the fluffy aerial hyphae (19), while those producing aerial hyphae but no spores are referred to as white (*whi*), as they fail to produce grey-pigmented spores (20).

The *Streptomyces* genome encodes a large number of cell wall-modifying enzymes, such as cell wall hydrolases (autolysins), carboxypeptidases and penicillin-binding proteins (PBPs), a complexity that suggests strong heterogeneity of the PG of these organisms (21, 22). Several concepts that were originally regarded as specific to eukaryotes also occur in bacteria, such as multicellularity (11, 23, 24) and programmed cell death (25, 26). Programmed cell death (PCD) likely plays a major role in the onset of morphological development, required to lyse part of the vegetative mycelium to provide the nutrients for the aerial hyphae (27, 28). PCD and cell-wall recycling are linked to antibiotic production in *Streptomyces* (29).

All disaccharide peptide subunits (muropeptides) in the PG are variations on the basic building block present in lipid II, which in *Streptomyces* typically consists of GlcNAc-MurNAc-L-Ala-D-Glu-LL-DAP(Gly)-D-Ala-D-Ala (30, 31). Here, we have analyzed the cell wall composition of vegetative mycelium and mature spores of *Streptomyces coelicolor* by LC-MS, to obtain a detailed inventory of the monomers and dimers in the cell wall. This revealed extensive cell-wall hydrolysis and remodeling during vegetative growth and highlights the difference in cell-wall composition between vegetative hyphae and spores.

RESULTS

To assess how growth and development translate to variations in the PG composition, we isolated the PG of *S. coelicolor* and analyzed the muropeptide profile during different growth phases in liquid-grown cultures, and of spores. In submerged cultures, *S. coelicolor* does not sporulate, while it forms aerial hyphae and spores on solid media. Vegetative mycelia of *S. coelicolor* M145 were harvested from cultures grown in liquid minimal media (NMM+). Samples taken after 18 h and 24 h represented exponential growth, while samples taken after 36 h and 48 h represented mycelia in transition phase (Figure 1A,B). Samples from solid-grown cultures were taken at 24 h to represent vegetative growth, 48 h, representing growth of aerial hyphae and 72 h, when the strain has formed spores (Figure 1C). Spores were harvested from SFM agar plates and filtered to exclude mycelial fragments.

To allow analyzing a large number of samples simultaneously and in a reasonable time frame, we adapted a method for PG purification (32) for use in *S. coelicolor*. The advantage of this method is that it requires only a small amount of input biomass and much faster sample handling. For this, 10 mg of lyophilized cell-wall material was isolated by boiling cells in 0.25% SDS in 2 ml microcentrifuge tubes, and secondary cell-wall polymers such as teichoic acids were removed by treatment for 4 h with hydrochloric acid (HCl) (see Materials and Methods section for details). As a control for the validity of the method, it was compared to a more elaborate method that is used more routinely (33). In the latter method, biomass from 1 L culture of *S. coelicolor* was boiled in 5% SDS and subsequently treated for 48 h with hydrofluoric acid (HF) to remove teichoic acids. Comparison of the two methods revealed comparable outcomes between the two methods in peak detection (Table S5). This validated the rapid method based on 0.25% SDS and HCl, which was therefore used in this study.

The isolated PG was digested with mutanolysin (32, 34) and the muropeptide composition was analyzed by liquid chromatography linked to mass spectrometry (LC-MS). Peaks were identified in the m/z range from 500-3000 Da, whereby different m/z in co-eluting peaks were further characterized by MS/MS. The eluted m/z values were compared to a

dataset of theoretical masses of predicted muropeptides. Table 1 shows a summary of the monomers and dimers that were detected during growth in liquid media, and Table 2 a summary of muropeptides during growth on solid media. The full datasets are given in Tables S1-S4. We identified several modifications, including the amidation of D-iGlu to D-iGln at position 2 of the stem peptide, deacetylation of MurNAc to MurN, removal of amino acids to generate mono-, di-, tri- and tetrapeptides, loss of LL-DAP-bound glycine, and the presence of Gly (instead of Ala) at position 1,4 or 5. The loss of GlcNac or GlcNAc-MurNAc indicates hydrolysis (Figure 2).

For all amino acid positions in the pentapeptide chain, the position is indicated as [n], whereby n is the number in the chain (with [1] the position closest to the PG backbone, i.e. the MurNac residue, and [5] the last aa residue).

Growth phase-dependent changes in the PG composition

The muropeptide that is incorporated from Lipid II by glycosyltransferases contains a pentapeptide with a Gly residue linked to LL-DAP in aa position 3 (LL-DAP[3]). In many bacteria pentapeptides are short-lived muropeptides that occur mostly at sites where *de novo* cell-wall synthesis takes place, *i.e.* during growth and division (35, 36). This is reflected by the high abundance of pentapeptides in the samples obtained from exponentially growing cells, with a pentapeptide content of 21% during early exponential growth (18 h), as compared to 14% and 11% during late exponential growth (24 h), transition phase (36 h) and stationary phase (48 h), respectively. Conversely, tripeptides increased over time, from 24% during early exponential phase to 32% in transition-phase cultures.

Addition of Gly to the medium and, in consequence, incorporation of Gly in the PG can cause changes in morphology (37, 38). This property has been applied to facilitate lysozyme-mediated formation of protoplasts in *Streptomyces*, used for protoplast transformation methods (39-41). In *S. coelicolor*, Gly can be found instead of D-Ala[1], D-Ala[4] or D-Ala[5] in the pentapeptide chain. During liquid growth, tetrapeptides carrying Gly[4] increased from 3% during early growth to 8% during the latest time points. The relative

157 abundance of pentapeptides carrying Gly at position 5 (4-5%) did not vary over time. On
158 solid-grown cultures, the Gly content of the peptidoglycan was around 1%, which is
159 significantly lower than in liquid-grown cultures.
160
161 **The abundance of 3-3 cross-links increases over time**
162 Two types of cross-links are formed via separate mechanisms, namely the canonical D,D-
163 transpeptidases (PBPs) producing 3-4 (D,D) cross-links between LL-DAP[3] and D-Ala[4] and
164 L,D-transpeptidases that form 3-3 (L,D) cross-links between two LL-DAP[3] residues (Figure
165 2). These types of peptidoglycan cross-linking can be distinguished based on differences in
166 retention time and their MS/MS fragmentation patterns. Dimers containing a tripeptide and a
167 tetrapeptide (TetraTri) may have either cross-link, giving rise to isomeric forms that elute at
168 different retention times, allowing for assessment by MS/MS (Figures 3A and 3B). In *S.*
169 *coelicolor*, the ratio of 3-3 cross-linking increased over time towards transition phase; the
170 relative abundance increased from 37% of the total amount of dimers at 18 h (exponential
171 phase) to 57% of all dimers at 48 h (Figures 3A and 3B).
172
173 **PG hydrolysis increases as the culture ages**
174 PG hydrolysis is associated with processes such as separation of daughter cells after cell
175 division and autolysis, and mutants of bacteria that fail to produce PG amidases grow in
176 chains of connected cells (42, 43). On solid media, vegetative hyphae of *Streptomyces*
177 undergo programmed cell death (PCD) and hydrolysis. In liquid-grown cultures, cell death
178 occurs in the center of dense pellets. During spore maturation, spores are separated
179 hydrolytically from one another. Some streptomycetes sporulate in submerged culture, but
180 this is not the case for *S. coelicolor* (44). Our data show that as growth proceeds in
181 submerged cultures, the *S. coelicolor* peptidoglycan progressively loses GlcNAc and
182 GlcNAc-MurNAc moieties (Table 1), as a result of N-acetylglucosaminidase activity. The
183 proportion of dimers lacking GlcNAc-MurNAc thereby increases in time from 24% at 18 h to
184 56% at 48 h. Figure 3C shows MS/MS profiles of a TriTri-dimer with a single set of glycans.

During growth on solid media the trend was inversed. This may be due to the different developmental stages, whereby 24 h corresponds to early developmental events and PCD, 48 h to aerial growth and sporulation at 72 h. This analysis shows the relative abundance of muropeptides of the total amount of biomass, when hydrolysis has occurred at the vegetative mycelium. During later stages of growth on agar plates a large amount of aerial hyphae is formed, and this can therefore not be compared directly to samples that only contain vegetative hyphae (Table 2).

Deacetylation of MurNAc is associated with mycelial aging and sporulation

Modifications to the glycan strands are commonly linked to lysozyme resistance (45). In particular, N-deacetylation of PG strands is widespread among bacteria, which can occur both at GlcNAc and at MurNAc (46). In the case of *S. coelicolor*, the only glycan modification is the deacetylation of MurNAc to MurN. Our data show that this modification becomes more prominent as the vegetative mycelium ages, from 5% during early growth to 8% during later growth stages. On agar plates, 3.7% of the monomers was deacetylated at 24 h, 4.4% at 48 h and 6.1% at 72 h.

The PG composition of spores and vegetative mycelia was compared to get more insights into the possible correlations between PG composition and important processes such as dormancy and germination. Muropeptides in spores were strongly biased for tetrapeptides, making up 44% of the monomers, as compared to 23-25% of the vegetative PG. Conversely, pentapeptides were found in much lower amounts in spores (5% of the monomers), as compared to 10-22% in vegetative hyphae. The muropeptide that stood out in the analysis of the spore PG was a tripeptide which lacks GlcNAc and contains a deacetylated MurNAc, called MurN-Tri (Figure 2). In spores, MurN-Tri made up 3.5% of the monomers, whereas the less modified muropeptide, GlcNAcMurN-Tri only made up 0.2% of the monomers.

To further investigate this interesting phenomenon, and show the applicability of our work for the analysis of developmental mutants, we analyzed *bldD* and *whiG* mutants. The

bldD gene product is a global transcription factor that controls the transcription of many developmental genes and is therefore blocked in an early stage of morphogenesis (47), while the *whiG* gene product is a σ factor that controls early events of aerial growth (48). The monomer profile of *S. coelicolor* M145 and its *bldD* and *whiG* mutants are summarized in Table 3. For the wild-type strain M145, 24 h represents vegetative growth, 48 h aerial growth and 72 h spore formation. In line with the notion that MurN-Tri accumulates particularly in spores, the *bldD* mutant accumulated hardly any MurN-Tri (0-0.2%) over the course of time and the *whiG* mutant 0.4%, 0.6% and 1.3% after 24 h, 48 h, and 72 h. respectively. In contrast, the wild-type strain M145 had 0.6%, 1.7% and 3.1% MurN-Tri at these time points, respectively, strongly suggesting that MurN-Tri accumulates in a sporulation-specific manner.

DISCUSSION

In this study we have analyzed changes in the composition of the peptidoglycan during growth and development of *Streptomyces coelicolor*. The different masses were thereby identified by MS and MS/MS analysis, which allowed detailed identification of the subunits, including dimers that are cross-linked by either 3-3 or 3-4 cross-links between the peptide moieties. Our data show that the *Streptomyces* peptidoglycan composition is changing dynamically, whereby major peptidoglycan recycling was seen, whereby over half of all GlcNAc-MurNac dimers were hydrolyzed in late-exponential cultures.

L,D-transpeptidases (LDTs) are especially prevalent in the actinobacterial genera *Mycobacterium*, *Corynebacterium* and *Streptomyces*. Suggestively, these bacteria have a much higher percentage of 3-3 cross-links, with an abundance of at least 30% 3-3-cross links in investigated actinobacterial peptidoglycan as compared to bacteria with lateral cell-wall growth such as *E. coli* (<10%) and *E. faecium* (3%) (30, 49, 50). LDTs attach to D-Ala[4] and form a cross-link between glycine and LL-DAP[3]. D-Ala[4] is considered a donor for this type of cross-link (51). An interesting feature of these two mechanisms is that 3-4 cross-links can

only be formed when a pentapeptide is present to display the D-Ala[5] donor, whereas 3-3 cross-links can be formed with a tetrapeptide as a donor strand. Dimers in vegetative (liquid-grown) cells carry 36.5% 3-3 cross-links at 18 h of growth, increasing to 48% at 24 h, 54.5% at 36 h and 57.3% at 48 h. Between these stages of growth, the main structural difference is the length of hyphae compared to growing tips. The data agrees with the idea that 3-3 cross-links could be required to remodel the cell wall beyond the tip-complex, using available tetrapeptides contrary to newly constructed pentapeptides (52-55).

A major event associated with lytic degradation of the cells is programmed cell death (PCD). PCD is likely a major hallmark of multicellularity (11), and has been described in the biofilm-forming *Streptococcus* (56) and *Bacillus* (57), in Myxobacteria that form fruiting bodies (58), in the filamentous cyanobacteria (59, 60), and in the branching *Streptomyces* (28, 61, 62). In streptomycetes, cell-wall hydrolases support developmental processes like branching and germination (21). Additionally, PCD and the autolytic release of GlcNAc from the cell wall is an important signal for the onset of morphological differentiation and antibiotic production in streptomycetes (29, 63). Our data show an exceptionally high amount of dimers which carry a cross-linked set of peptides but a single set of glycans, from 25% of dimers in 18 h old liquid cultures to 56% at 48 h old cultures. The increase in abundance of dimers lacking a set of glycans is especially prevalent in liquid-grown mycelia, while the overall increase in hydrolyzed dimers is not as high in mycelia grown on solid media. It should ne noted that on agar plates also aerial hyphae are formed, which are not subject to the extensive lysis seen in vegetative hyphae, and this may reduce the relative content of these glycan-less peptides.

We have also analyzed changes in the PG that correlate to sporulation. One question that remains to be answered is how future sites of branching in the hyphae or germination in the spores are marked, and oen interesting possibility the cell wall may be changed as a marker for the start of future *de novo* PG synthesis. After all, even after very long storage of spores, germination still occurs at the spore 'poles', suggesting that physical marks to the PG, such as rare modifications, may occur. A previous study showed that mutation of the

gene *dacA* that encodes D-alanyl-D-alanine carboxypeptidase disrupts spore maturation and germination, where one could influence the other. This indicates that either pentapeptides inhibit spore maturation, or that a high amount of tetrapeptides is important (64). Indeed, we report a high amount of tetrapeptides in spores, 48% of the monomers. A necessity for tetrapeptides could be linked to the formation of 3-3 cross-links, which require tetrapeptides, contrary to pentapeptides, as a substrate. Indeed, spores carry 3-3 cross-links in 35% of the dimers, which probably strongly contribute to structural stability. Interestingly, a relatively high amount of MurN-Tri (3.5%) was identified in the spore PG, while this molecule was almost completely absent in *bldD* mutants, which are arrested in the vegetative growth phase. A small amount of MurN-Tri (0.4-1.2%) was found in *whiG* mutants, which do develop aerial hyphae but do not sporulate. It will be interesting to see what the biological significance is of the overrepresentation of MurN-Tri in aerial and spore PG. This underlines the importance of analyzing the cell wall of different culture types, as it reveals novel features that may play a key role in development.

CONCLUSIONS

We have provided a detailed analysis of the peptidoglycan of *Streptomyces* mycelia and spores, and developed a reliable and fast method to compare larger numbers of samples. Our data show significant changes over time, among which changes in the amino acid chain, hydrolysis of dimers, and the accumulation of the rare MurN-Tri specifically in the spores. The cell wall likely plays a major role in the development of streptomycetes, with implications for germination and the switch to development and antibiotic production (via PCD-released cell wall components). The dynamic process that controls the remodeling of the cell wall during tip growth is poorly understood, but we anticipate that the local cell-wall structure at sites of growth and branching may well be different from that in older (non-growing) hyphae. This is consistent with the changes we observed over time, between the younger and older mycelia. Detailed localization of cell-wall modifying enzymes and of specific cell-wall

296 modifications, in both time and space, should provide further insights into the role of the cell
297 wall in the control of growth and development of streptomycetes.

EXPERIMENTAL PROCEDURES

Bacterial strain and culturing conditions

Streptomyces coelicolor A3(2) M145 (41), *bldD* mutant J774 (*cysA15 pheA1 mthB2 bldD53* NF SCP2* (19)) and *whiG* mutant J2400 (*whiG*::*hyg* (65)), were obtained from the John Innes Centre strain collection. All media and methods for handling *Streptomyces* are described in the *Streptomyces* laboratory manual (41). Spores were collected from Soy Flour Mannitol (SFM) agar plates. Liquid cultures were grown shaking at 30°C in a flask with a spring, using normal minimal medium with phosphate (NMM+) supplemented with 1% (w/v) mannitol as the sole carbon source; polyethylene glycol (PEG) was omitted to avoid interference with the MS identification. Cultures were inoculated with spores at a density of 10^6 CFU/ML. A growth curve was constructed from dry-weight measurements by freeze-drying washed biomass obtained from 10 ml of culture broth (three biological replicates). To facilitate the harvest of mycelium from agar plates, they were grown on cellophane slips, after which the biomass was scraped of the cellophane. Spores were collected from SFM agar plates by adding 0.01% (w/v) SDS to facilitate spore release from the aerial mycelium, scraping them off with a cotton ball and drawing the solution with a syringe. Spores were filtered with a cotton filter to separate spores from residual mycelium.

PG extraction

Cells were lyophilized for a biomass measurement, 10 mg biomass was directly used for PG isolation. PG was isolated according to (32), using 2 mL screw-cap tubes for the entire isolation. Biomass was first boiled in 0.25% SDS in 0.1 M Tris/HCl pH 6.8, thoroughly washed, sonicated, treated with DNase, RNase and trypsin, inactivation of proteins by boiling and washing with water. Wall teichoic acids were removed with 1 M HCl. PG was digested with mutanolysin and lysozyme (66). Muropeptides were reduced with sodium borohydride and the pH was adjusted to 3.5-4.5 with phosphoric acid.

To validate the method, we compared it to the method described previously (33). For this, *S. coelicolor* mycelia were grown in 1 L NMM+ media for 24 h. After washing of the

mycelia, pellets were resuspended in boiling 5% (w/v) SDS and stirred vigorously for 20 min. Instead of sonicating the cells, they were disrupted using glass beads, followed by removal of the teichoic acids with an HF treatment at 4°C as described.

LC-MS analysis of monomers

The LC-MS setup consisted of a Waters Acquity UPLC system (Waters, Milford, MA, USA) and a LTQ Orbitrap XL Hybrid Ion Trap-Orbitrap Mass Spectrometer (Thermo Fisher Scientific, Waltham, MA, USA) equipped with an Ion Max electrospray source. Chromatographic separation was performed on an Acquity UPLC HSS T3 C_{18} column (1.8 µm, 100 Å, 2.1 × 100 mm). Mobile phase A consist of 99.9% H_2O and 0,1% Formic Acid and mobile phase B consists of 95% Acetonitrile, 4.9% H_2O and 0,1% Formic Acid. All solvents used were of LC-MS grade or better. The flow rate was set to 0.5 ml/min. The binary gradient program consisted of 1 min 98% A, 12 min from 98% A to 85% A, and 2 min from 85% A to 0% A. The column was then flushed for 3 min with 100% B, the gradient was then set to 98% A and the column was equilibrated for 8 min. The column temperature was set to 30°C and the injection volume used was 5 µL. The temperature of the autosampler tray was set to 8°C. Samples were run in triplicates.

MS/MS was done both on the full chromatogram by data dependent MS/MS and on specific peaks by selecting the mass of interest. Data dependent acquisition was performed on the most intense detected peaks, the activation type was Collision Induced Dissociation (CID). Selected MS/MS was performed when the resolution of a data dependent acquisition lacked decisive information. MS/MS experiments in the ion trap were carried out with relative collision energy of 35% and the trapping of product ions were carried out with a q-value of 0.25, and the product ions were analyzed in the ion trap., data was collected in the positive ESI mode with a scan range of *m/z* 500–3000 in high range mode. The resolution was set to 15.000 (at m/z 400).

Data analysis

Chromatograms were evaluated using the free software package MZmine (http://mzmine.sourceforge.net/ (67)) to detect peaks, deconvolute the data and align the peaks. Only peaks corresponding with a mass corresponding to a muropeptide were saved, other data was discarded. The online tool MetaboAnalyst (68) was used to normalize the data by the sum of the total peak areas, then normalize the data by log transformation. The normalized peak areas were exported and a final table which shows peak areas as percentage of the whole was produced in Microsoft Excel.

Muropeptide identification

The basic structure of the peptidoglycan of *S. coelicolor* has been published previously (30). Combinations of modifications were predicted and the masses were calculated using ChemDraw Professional (PerkinElmer). When a major peak had an unexpected mass, MS/MS helped resolve the structure. MS/MS was used to identify differences in cross-linking and to confirm predicted structures.

Acknowledgments

This work is part of the profile area Antibiotics of the Faculty of Sciences of Leiden University.

Conflict of interest statement

The authors declare that they have no conflicts of interest with the contents of this article.

Author contributions

LvdA performed the experiments with the help of GS. LvdA and GvW conceived the study. LvdA, AH, TH and GvW wrote the article with the help of WV. All authors approved the final manuscript.

REFERENCES

1. Vollmer W, Blanot D, de Pedro MA. 2008. Peptidoglycan structure and architecture. FEMS Microbiol Rev 32:149-67.
2. Kysela DT, Randich AM, Caccamo PD, Brun YV. 2016. Diversity Takes Shape: Understanding the Mechanistic and Adaptive Basis of Bacterial Morphology. PLoS Biol 14:e1002565.
3. Egan AJ, Cleverley RM, Peters K, Lewis RJ, Vollmer W. 2017. Regulation of bacterial cell wall growth. FEBS J 284:851-867.
4. Leclercq S, Derouaux A, Olatunji S, Fraipont C, Egan AJ, Vollmer W, Breukink E, Terrak M. 2017. Interplay between Penicillin-binding proteins and SEDS proteins promotes bacterial cell wall synthesis. Sci Rep 7:43306.
5. Sham LT, Butler EK, Lebar MD, Kahne D, Bernhardt TG, Ruiz N. 2014. Bacterial cell wall. MurJ is the flippase of lipid-linked precursors for peptidoglycan biogenesis. Science 345:220-2.
6. Popham DL. 2002. Specialized peptidoglycan of the bacterial endospore: the inner wall of the lockbox. Cell Mol Life Sci 59:426-33.
7. Keep NH, Ward JM, Cohen-Gonsaud M, Henderson B. 2006. Wake up! Peptidoglycan lysis and bacterial non-growth states. Trends Microbiol 14:271-6.
8. Barka EA, Vatsa P, Sanchez L, Gavaut-Vaillant N, Jacquard C, Meier-Kolthoff J, Klenk HP, Clément C, Oudouch Y, van Wezel GP. 2016. Taxonomy, physiology, and natural products of the *Actinobacteria*. Microbiol Mol Biol Rev 80:1-43.
9. Celler K, Koning RI, Willemse J, Koster AJ, van Wezel GP. 2016. Cross-membranes orchestrate compartmentalization and morphogenesis in *Streptomyces*. Nat Comm 7:11836.
10. Flärdh K, Buttner MJ. 2009. *Streptomyces* morphogenetics: dissecting differentiation in a filamentous bacterium. Nat Rev Microbiol 7:36-49.
11. Claessen D, Rozen DE, Kuipers OP, Sogaard-Andersen L, van Wezel GP. 2014. Bacterial solutions to multicellularity: a tale of biofilms, filaments and fruiting bodies. Nat Rev Microbiol 12:115-24.
12. Jakimowicz D, van Wezel GP. 2012. Cell division and DNA segregation in *Streptomyces*: how to build a septum in the middle of nowhere? Mol Microbiol 85:393-404.
13. Wolanski M, Wali R, Tilley E, Jakimowicz D, Zakrzewska-Czerwinska J, Herron P. 2011. Replisome trafficking in growing vegetative hyphae of *Streptomyces coelicolor* A3(2). J Bacteriol 193:1273-5.
14. van Dissel D, Claessen D, Van Wezel GP. 2014. Morphogenesis of *Streptomyces* in submerged cultures. Adv Appl Microbiol 89:1-45.
15. McCormick JR. 2009. Cell division is dispensable but not irrelevant in *Streptomyces*. Curr Opin Biotechnol 12:689-98.
16. Noens EE, Mersinias V, Traag BA, Smith CP, Koerten HK, van Wezel GP. 2005. SsgA-like proteins determine the fate of peptidoglycan during sporulation of *Streptomyces coelicolor*. Mol Microbiol 58:929-44.
17. Celler K, Koning RI, Koster AJ, van Wezel GP. 2013. Multidimensional view of the bacterial cytoskeleton. J Bacteriol 195:1627-36.
18. Holmes NA, Walshaw J, Leggett RM, Thibessard A, Dalton KA, Gillespie MD, Hemmings AM, Gust B, Kelemen GH. 2013. Coiled-coil protein Scy is a key component of a multiprotein assembly controlling polarized growth in *Streptomyces*. Proc Natl Acad Sci U S A 110:E397-406.
19. Merrick MJ. 1976. A morphological and genetic mapping study of bald colony mutants of *Streptomyces coelicolor*. J Gen Microbiol 96:299-315.
20. Chater KF. 1972. A morphological and genetic mapping study of white colony mutants of *Streptomyces coelicolor*. J Gen Microbiol 72:9-28.
21. Haiser HJ, Yousef MR, Elliot MA. 2009. Cell wall hydrolases affect germination, vegetative growth, and sporulation in *Streptomyces coelicolor*. J Bacteriol 191:6501-12.

22. Peters K, Kannan S, Rao VA, Biboy J, Vollmer D, Erickson SW, Lewis RJ, Young KD, Vollmer W. 2016. The Redundancy of Peptidoglycan Carboxypeptidases Ensures Robust Cell Shape Maintenance in *Escherichia coli*. MBio 7.
23. Lyons NA, Kolter R. 2015. On the evolution of bacterial multicellularity. Curr Opin Microbiol 24:21-8.
24. Shapiro JA. 1988. Bacteria as multicellular organisms. Sci Am 256:82-89.
25. Hochman A. 1997. Programmed cell death in prokaryotes. Crit Rev Microbiol 23:207-14.
26. Rice KC, Bayles KW. 2003. Death's toolbox: examining the molecular components of bacterial programmed cell death. Mol Microbiol 50:729-38.
27. Manteca A, Fernandez M, Sanchez J. 2005. Mycelium development in *Streptomyces antibioticus* ATCC11891 occurs in an orderly pattern which determines multiphase growth curves. BMC microbiology 5:51.
28. Miguelez EM, Hardisson C, Manzanal MB. 1999. Hyphal death during colony development in Streptomyces antibioticus: morphological evidence for the existence of a process of cell deletion in a multicellular prokaryote. J Cell Biol 145:515-25.
29. Urem M, Swiatek-Polatynska MA, Rigali S, van Wezel GP. 2016. Intertwining nutrient-sensory networks and the control of antibiotic production in Streptomyces. Mol Microbiol 102:183-195.
30. Hugonnet JE, Haddache N, Veckerle C, Dubost L, Marie A, Shikura N, Mainardi JL, Rice LB, Arthur M. 2014. Peptidoglycan cross-linking in glycopeptide-resistant *Actinomycetales*. Antimicrob Agents Chemother 58:1749-56.
31. Schleifer KH, Kandler O. 1972. Peptidoglycan Types of Bacterial Cell-Walls and Their Taxonomic Implications. Bacteriol Rev 36:407-477.
32. Kühner D, Stahl M, Demircioglu DD, Bertsche U. 2014. From cells to muropeptide structures in 24 h: peptidoglycan mapping by UPLC-MS. Sci Rep 4:7494.
33. Bui NK, Eberhardt A, Vollmer D, Kern T, Bougault C, Tomasz A, Simorre JP, Vollmer W. 2012. Isolation and analysis of cell wall components from *Streptococcus pneumoniae*. Anal Biochem 421:657-66.
34. Glauner B. 1988. Separation and quantification of muropeptides with high-performance liquid chromatography. Anal Biochem 172:451-64.
35. Kuru E, Tekkam S, Hall E, Brun YV, Van Nieuwenhze MS. 2015. Synthesis of fluorescent D-amino acids and their use for probing peptidoglycan synthesis and bacterial growth in situ. Nat Protoc 10:33-52.
36. Morales Angeles D, Liu Y, Hartman AM, Borisova M, de Sousa Borges A, de Kok N, Beilharz K, Veening JW, Mayer C, Hirsch AK, Scheffers DJ. 2017. Pentapeptide-rich peptidoglycan at the *Bacillus subtilis* cell-division site. Mol Microbiol 104:319-333.
37. Hammes W, Schleifer KH, Kandler O. 1973. Mode of action of glycine on the biosynthesis of peptidoglycan. J Bacteriol 116:1029-53.
38. Takacs CN, Hocking J, Cabeen MT, Bui NK, Poggio S, Vollmer W, Jacobs-Wagner C. 2013. Growth medium-dependent glycine incorporation into the peptidoglycan of Caulobacter crescentus. PLoS One 8:e57579.
39. Okanishi M, Suzuki K, Umezawa H. 1974. Formation and reversion of *Streptomycete* protoplasts: cultural condition and morphological study. J Gen Microbiol 80:389-400.
40. Hopwood DA, Wright HM, Bibb MJ, Cohen SN. 1977. Genetic recombination through protoplast fusion in *Streptomyces*. Nature 268:171-4.
41. Kieser T, Bibb MJ, Buttner MJ, Chater KF, Hopwood DA. 2000. Practical *Streptomyces* genetics. John Innes Foundation, Norwich, U.K.
42. Heidrich C, Ursinus A, Berger J, Schwarz H, Holtje JV. 2002. Effects of multiple deletions of murein hydrolases on viability, septum cleavage, and sensitivity to large toxic molecules in *Escherichia coli*. J Bacteriol 184:6093-9.
43. Vollmer W, Joris B, Charlier P, Foster S. 2008. Bacterial peptidoglycan (murein) hydrolases. FEMS Microbiol Rev 32:259-86.

44. Girard G, Traag BA, Sangal V, Mascini N, Hoskisson PA, Goodfellow M, van Wezel GP. 2013. A novel taxonomic marker that discriminates between morphologically complex actinomycetes. Open Biol 3:130073.
45. Meyrand M, Boughammoura A, Courtin P, Mezange C, Guillot A, Chapot-Chartier MP. 2007. Peptidoglycan N-acetylglucosamine deacetylation decreases autolysis in *Lactococcus lactis*. Microbiology 153:3275-85.
46. Vollmer W. 2008. Structural variation in the glycan strands of bacterial peptidoglycan. FEMS Microbiol Rev 32:287-306.
47. den Hengst CD, Tran NT, Bibb MJ, Chandra G, Leskiw BK, Buttner MJ. 2010. Genes essential for morphological development and antibiotic production in *Streptomyces coelicolor* are targets of BldD during vegetative growth. Mol Microbiol 78:361-79.
48. Chater KF, Bruton CJ, Plaskitt KA, Buttner MJ, Mendez C, Helmann JD. 1989. The developmental fate of *S. coelicolor* hyphae depends upon a gene product homologous with the motility sigma factor of *B. subtilis*. Cell 59:133-43.
49. Cameron TA, Anderson-Furgeson J, Zupan JR, Zik JJ, Zambryski PC. 2014. Peptidoglycan synthesis machinery in *Agrobacterium tumefaciens* during unipolar growth and cell division. MBio 5:e01219-14.
50. Lavollay M, Arthur M, Fourgeaud M, Dubost L, Marie A, Riegel P, Gutmann L, Mainardi JL. 2009. The beta-lactam-sensitive D,D-carboxypeptidase activity of Pbp4 controls the L,D and D,D transpeptidation pathways in *Corynebacterium jeikeium*. Mol Microbiol 74:650-61.
51. Mainardi JL, Fourgeaud M, Hugonnet JE, Dubost L, Brouard JP, Ouazzani J, Rice LB, Gutmann L, Arthur M. 2005. A novel peptidoglycan cross-linking enzyme for a beta-lactam-resistant transpeptidation pathway. J Biol Chem 280:38146-52.
52. Lavollay M, Arthur M, Fourgeaud M, Dubost L, Marie A, Veziris N, Blanot D, Gutmann L, Mainardi JL. 2008. The peptidoglycan of stationary-phase *Mycobacterium tuberculosis* predominantly contains cross-links generated by L,D-transpeptidation. J Bacteriol 190:4360-6.
53. Sanders AN, Wright LF, Pavelka MS, Jr. 2014. Genetic characterization of mycobacterial L,D-transpeptidases. Microbiology 160:1795-806.
54. Sacco E, Hugonnet JE, Josseaume N, Cremniter J, Dubost L, Marie A, Patin D, Blanot D, Rice LB, Mainardi JL, Arthur M. 2010. Activation of the L,D-transpeptidation peptidoglycan cross-linking pathway by a metallo-D,D-carboxypeptidase in *Enterococcus faecium*. Mol Microbiol 75:874-85.
55. Baranowski C, Sham L-T, Eskandarian HA, Welsh MA, Lim HC, Kieser KJ, Wagner JC, Walker S, McKinney JD, Fantner GE, Ioerger TR, Bernhardt TG, Rubin EJ, Rego EH. 2018. Maturing Mycobacterial Peptidoglycan Requires Non-canonical Crosslinks to Maintain Shape. bioRxiv.
56. Guiral S, Mitchell TJ, Martin B, Claverys JP. 2005. Competence-programmed predation of noncompetent cells in the human pathogen *Streptococcus pneumoniae*: genetic requirements. Proc Natl Acad Sci U S A 102:8710-5.
57. Engelberg-Kulka H, Amitai S, Kolodkin-Gal I, Hazan R. 2006. Bacterial programmed cell death and multicellular behavior in bacteria. PLoS Genet 2:e135.
58. Sogaard-Andersen L, Yang Z. 2008. Programmed cell death: role for MazF and MrpC in *Myxococcus* multicellular development. Curr Biol 18:R337-9.
59. Bornikoel J, Carrion A, Fan Q, Flores E, Forchhammer K, Mariscal V, Mullineaux CW, Perez R, Silber N, Wolk CP, Maldener I. 2017. Role of Two Cell Wall Amidases in Septal Junction and Nanopore Formation in the Multicellular *Cyanobacterium Anabaena* sp. PCC 7120. Front Cell Infect Microbiol 7:386.
60. Ning SB, Guo HL, Wang L, Song YC. 2002. Salt stress induces programmed cell death in prokaryotic organism Anabaena. J Appl Microbiol 93:15-28.
61. Manteca A, Mader U, Connolly BA, Sanchez J. 2006. A proteomic analysis of *Streptomyces coelicolor* programmed cell death. Proteomics 6:6008-22.

62. Tenconi E, Traxler MF, Hoebreck C, van Wezel GP, Rigali S. 2018. Production of prodiginines Is part of a programmed cell death process in *Streptomyces coelicolor*. Frontiers Microbiol:in press.
63. Rigali S, Titgemeyer F, Barends S, Mulder S, Thomae AW, Hopwood DA, van Wezel GP. 2008. Feast or famine: the global regulator DasR links nutrient stress to antibiotic production by *Streptomyces*. EMBO Rep 9:670-5.
64. Rioseras B, Yague P, Lopez-Garcia MT, Gonzalez-Quinonez N, Binda E, Marinelli F, Manteca A. 2016. Characterization of SCO4439, a D-alanyl-D-alanine carboxypeptidase involved in spore cell wall maturation, resistance, and germination in *Streptomyces coelicolor*. Sci Rep 6:21659.
65. Flärdh K, Findlay KC, Chater KF. 1999. Association of early sporulation genes with suggested developmental decision points in *Streptomyces coelicolor* A3(2). Microbiology 145:2229-43.
66. Arbeloa A, Hugonnet JE, Sentilhes AC, Josseaume N, Dubost L, Monsempes C, Blanot D, Brouard JP, Arthur M. 2004. Synthesis of mosaic peptidoglycan cross-bridges by hybrid peptidoglycan assembly pathways in gram-positive bacteria. J Biol Chem 279:41546-56.
67. Pluskal T, Castillo S, Villar-Briones A, Oresic M. 2010. MZmine 2: modular framework for processing, visualizing, and analyzing mass spectrometry-based molecular profile data. BMC Bioinformatics 11:395.
68. Xia J, Sinelnikov IV, Han B, Wishart DS. 2015. MetaboAnalyst 3.0--making metabolomics more meaningful. Nucleic Acids Res 43:W251-7.

558 **LEGENDS**

559

560 **Figure 1.** Growth of *S. coelicolor* in liquid media (top) and on solid media (bottom). A: Growth
561 curve on NMM+ medium based on triplicate dry-weight measurements. B: Pellet morphology
562 in liquid media. After spore germination, hyphae emerge through top growth and branching
563 that form an intricate network or pellet. The center of pellets eventually lyses due to PCD
564 (light grey). C: Growth on solid media, starting with the development of vegetative mycelium
565 from a single spore; after the onset of development, the vegetative hyphae differentiate into
566 aerial hyphae that grow into the air, coinciding with lysis of the vegetative mycelium (zone of
567 lysis represented in light grey). Chains of spores are generated by septation of the aerial
568 hyphae.

569

570 **Figure 2.** Summary of structures of main monomers and dimers observed in PG from *S.*
571 *coelicolor*. Modification to the PG include: alteration of the length of the amino acid chain;
572 [Gly1], L-Ala is replaced by Gly; [Glu], where Glutamic acid (Glu) is present instead of D-
573 Glutamine (Gln); [Gly4], where D-Ala(4) is replaced by Gly; [Gly5], where D-Ala(5) is
574 replaced by Gly. Specific for dimers: (3-3) shows a cross-link between LL-DAP(3) to LL-
575 DAP(3) with a Gly-bridge; (3-4) shows a cross-link between LL-DAP(3) and D-Ala(4) with a
576 Gly-bridge; (-MurNAcGlcNAc) shows hydrolysis of a set of sugars.

577

578 **Figure 3.** MS/MS fragmentations of TetraTri dimers with either 3-3 cross-link (A) or 3-4
579 cross-link (B). Differentiation between these two types of cross-links is possible at the point
580 of asymmetry, at Gly attached to LL-DAP. The 3-3 cross-linked dimer (A) fragments into
581 masses of 966.0 m/z and 941.3 m/z, which can be found in the respective MS/MS spectrum.
582 The 3-4 cross-linked dimer (B) fragments into masses of 1037.4 m/z and 870.5 m/z. These
583 masses are found in the MS/MS spectrum. Boxed MS/MS spectra show a magnification of
584 masses between m/z 850 and 1050 to show masses present in lower abundance. (C) a TriTri

dimer lacking GlcNAcMurNAc with an M+H of 1355.6, diagnostic fragments are given in the proposed structures.

589 **Table 1.** Relative abundance(%)[a] of muropeptides in vegetative cells from liquid NMM+.

	***S. coelicolor* M145**			
Monomers[b]	**18 h**	**24 h**	**36 h**	**48 h**
Mono	1.6	2.1	3.3	3.3
Di	14.2	15.5	14.5	13.2
Tri	27.4	32.2	35.1	35.8
Tetra	26.7	24.4	23.9	23.9
Tetra[Gly4][c]	3.5	5.3	6.9	8.2
Penta	22.7	16.9	13.1	12.9
Penta[Gly5][c]	4.7	4.8	4.7	4.4
D-Glutamine	67	62	61.1	63.7
Deacetylated	3.9	6.0	7.9	8.0
MurN-Tri	0.1	0.7	1.2	2.3
GlcNAc-MurN-Tri	1.8	2.2	2.6	2.1
	***S. coelicolor* M145**			
Dimers[b]	**18 h**	**24 h**	**36 h**	**48 h**
TriTri (3-3)	4.1	4.8	6.5	7.0
TriTri - MurNAcGlcNAc	8.7	14.8	23.7	34.3
TriTetra(3-3)	23.9	24.2	22.3	16.9
TriTetra(3-4)	1.0	8.7	8.2	6.1
TriTetra - MurNAcGlcNAc	9.6	15.1	16.1	16.2
TetraTetra(3-4)	23.3	13.5	10.1	8.6
TetraTetra - MurNAcGlcNAc	6.0	7.3	4.8	5.6
TetraPenta (3-4)	24.6	9.1	5.6	3.0
MurN	1.8	1.2	1.5	1.2
-GlcNac	0.3	0.6	1.1	1.2
missing MurNAcGlcNAc	24.3	37.2	44.6	56.1
Proportion(%) of 3-3 cross-links	36.5	48.0	54.5	57.3

590 [a]Relative abundance is calculated as the ratio of the peak area over the sum of all peak
591 areas recognized in the chromatogram. [b]Monomers and dimers are treated as separate
592 datasets. [c] Gly detected instead of Ala

593

Table 2. Relative abundance(%)[a] of muropeptides in mycelia and spores of *S. coelicolor* M145 harvested after growth on SFM agar plates.

	***S. coelicolor* M145**			
Monomers[b]	**24 h**	**48 h**	**72 h**	**spores**
Mono	3.6	4.3	4.1	4.5
Di	21.6	17.6	17.9	13.1
Tri	29.6	34.3	34.2	28.1
Tetra	25.4	29.5	32.0	48.3
Tetra[Gly4][c]	0.9	1.1	1.0	2.3
Penta	16.8	9.9	7.2	5.3
Penta[Gly5][c]	1.2	1.4	1.3	4.0
Deacatylated	3.7	4.4	6.1	4.5
D-Glutamine	76.2	80.3	82.9	74.0
Missing GlcNAc	1.5	3.4	5.0	4.8
MurN-Tri	0.6	1.7	3.1	3.5
GlcNAc-MurN-Tri	1.9	1.4	1.6	0.1
	***S. coelicolor* M145**			
Dimers[b]	**24 h**	**48 h**	**72 h**	**spores**
Tri-Tri (3-3)	7.4	10.5	12.6	4.9
Tri-Tri - MurNacGlcNac	0.6	0.6	0.3	7.1
Tri-Tetra(3-3)	20.4	22.2	21.8	19.1
Tri-Tetra(3-4)	9.7	12.7	11.8	4.7
Tri-Tetra - MurNacGlcNac	13.3	14.5	13.0	6.3
Tetra-Tetra(3-4)	13.3	15.8	15.7	38.9
Tetra-Tetra - MurNacGlcNac	17.3	13.7	13.2	17.1
Tetra-Penta (3-4)	12.7	7.3	5.4	0.7
MurN	1.0	0.3	1.2	0.4
-GlcNAc	0.4	0.2	0.4	0.1
missing MurNAcGlcNAc	31.1	28.7	26.5	30.4
Proportion(%) of 3-3 cross-links	43.8	47.8	51.1	35.1

[a]Relative abundance is calculated as the ratio of the peak area over the sum of all peak areas recognized in the chromatogram. [b]Monomers and dimers are treated as separate datasets. [c] Gly detected instead of Ala

600 **Table 3.** Relative abundance (in %)[a] of monomers from developmental *bldD* and *whiG*

601 mutants and the wild-type strain, *S. coelicolor* M145.

		Mono	Di	Tri	Tetra	Penta	Deacetylated	MurN-Tri	GlcNAc-MurN-Tri
Δ*bldD*	**24 h**	4.5	25.7	28.0	23.0	10.8	6.5	0.0	5.3
	48 h	4.3	26.3	38.3	23.4	11.1	8.5	0.2	6.6
	72 h	4.3	27.2	40.9	19.9	9.5	7.6	0.2	5.8
Δ*whiG*	**24 h**	3.5	23.2	27.0	32.5	15.2	3.0	0.4	1.3
	48 h	3.6	17.5	44.3	25.5	7.9	5.0	0.6	3.2
	72 h	4.1	18.5	48.8	20.9	6.9	6.2	1.3	3.8
M145 (wt)	**24 h**	3.6	21.6	29.6	25.4	16.8	3.7	0.6	1.9
	48 h	4.3	17.6	34.3	29.5	9.9	4.4	1.7	1.4
	72 h	4.1	17.9	34.2	32.0	7.2	6.1	3.1	1.6
spores		4.5	13.1	28.1	48.3	5.3	4.5	3.5	0.1

602 [a] Relative abundance is calculated as the ratio of the peak area over the sum of all peak

603 areas recognized in the chromatogram.

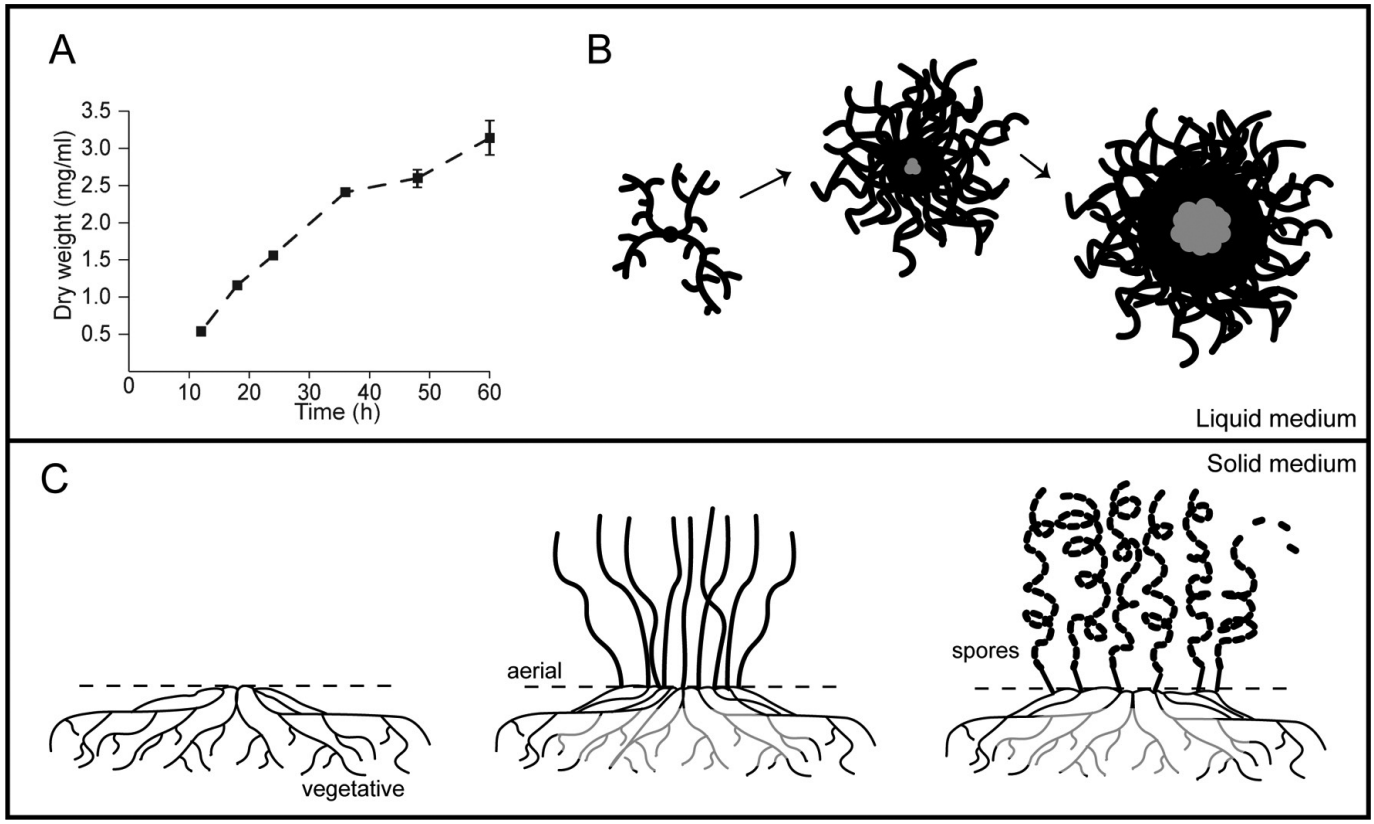

Monomers

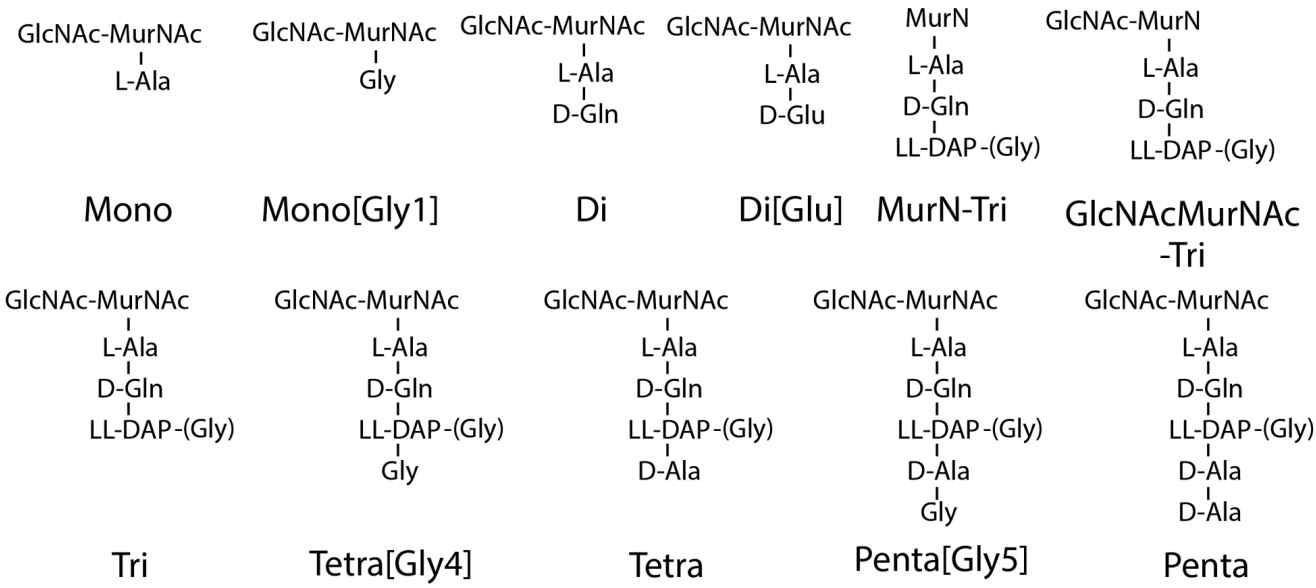

Dimers